Central α-Klotho Suppresses NPY/AgRP Neuron Activity and Regulates Metabolism in Mice

Taylor Landry,[1,2,3] Brenton Thomas Laing,[1,2,3] Peixin Li,[1,2,3] Wyatt Bunner,[1,2,3] Zhijian Rao,[1,2,3] Amber Prete,[1,3] Julia Sylvestri,[1,2,3] and Hu Huang[1,2,3,4]

α-Klotho is a circulating factor with well-documented antiaging properties. However, the central role of α-klotho in metabolism remains largely unexplored. The current study investigated the potential role of central α-klotho to modulate neuropeptide Y/agouti-related peptide (NPY/AgRP)-expressing neurons, energy balance, and glucose homeostasis. Intracerebroventricular administration of α-klotho suppressed food intake, improved glucose profiles, and reduced body weight in mouse models of type 1 and 2 diabetes. Furthermore, central α-klotho inhibition via an anti–α-klotho antibody impaired glucose tolerance. Ex vivo patch clamp electrophysiology and immunohistochemical analysis revealed that α-klotho suppresses NPY/AgRP neuron activity, at least in part, by enhancing miniature inhibitory postsynaptic currents. Experiments in hypothalamic GT1-7 cells observed that α-klotho induces phosphorylation of AKT^{ser473}, ERK$^{thr202/tyr204}$, and FOXO1^{ser256} as well as blunts AgRP gene transcription. Mechanistically, fibroblast growth factor receptor 1 (FGFR1) inhibition abolished the downstream signaling of α-klotho, negated its ability to modulate NPY/AgRP neurons, and blunted its therapeutic effects. Phosphatidylinositol 3 kinase (PI3K) inhibition also abolished α-klotho's ability to suppress food intake and improve glucose clearance. These results indicate a prominent role of hypothalamic α-klotho/FGFR1/PI3K signaling in the modulation of NPY/AgRP neuron activity and maintenance of energy homeostasis, thus providing new insight into the pathophysiology of metabolic disease.

α-Klotho, a well-documented antiaging protein primarily produced in the kidney and choroid plexus (1,2), has recently been observed to have therapeutic potential in rodent models of metabolic disease (3–6). Studies show α-klotho promotes lipid oxidation, protects pancreatic β-cells from oxidative damage, increases energy expenditure, and facilitates insulin release (3–7). Furthermore, circulating α-klotho concentrations are decreased in patients with obesity and diabetes (8), suggesting a possible direct role in the pathophysiology of metabolic disorders. Notably, studies have primarily investigated peripheral α-klotho, which neglects the central function of α-klotho due to its impermeability to the blood-brain barrier (9). The few studies investigating centrally circulating α-klotho demonstrate that α-klotho has antioxidative and anti-inflammatory properties (10), is involved in myelination (11), and can be therapeutic in models of hypertension (12). However, the role of central α-klotho in the regulation of metabolism remains unexplored.

Neuropeptide Y/agouti-related peptide (NPY/AgRP)-expressing neurons are located within the arcuate nucleus (ARC) of the hypothalamus and are critical to homeostatic regulation of metabolism. NPY/AgRP neurons sense nutritional changes in the cerebrospinal fluid (CSF) to regulate feeding behavior (13), energy expenditure (14), and glucose metabolism (15–17). However, disordered overactivity of these neurons results in phenotypes resembling diabetes and obesity (13,15). Some circulating factors, such as leptin and insulin, also modulate NPY/AgRP neurons (18,19), but in metabolic disease states, signaling of these hormones is disrupted. Therefore, identification of novel regulators of this neuron population could facilitate the development of therapeutic tools for the prevention and treatment of metabolic disease.

[1]East Carolina Diabetes and Obesity Institute, East Carolina University, Greenville, NC

[2]Department of Kinesiology, East Carolina University, Greenville, NC

[3]Human Performance Laboratory, College of Human Performance and Health, East Carolina University, Greenville, NC

[4]Department of Physiology, East Carolina University, Greenville, NC

Corresponding author: Hu Huang, huangh@ecu.edu

This article contains supplementary material online at https://doi.org/10.2337/db20-4567/suppl.12129981.

METABOLISM

Recent studies have identified several fibroblast growth factor (FGF) hormones that activate FGF receptor (FGFR)–phosphatidylinositol 3 kinase (PI3K) signaling to elicit antidiabetic effects and regulate NPY/AgRP neurons (20–25). Interestingly, α-klotho serves as a critical scaffolding protein to the FGF23-FGFR complex to promote FGFR activity (26,27). The current study investigates the novel role of central α-klotho in the regulation of NPY/AgRP neurons and whole-body metabolism via an FGFR/PI3K mechanism.

RESEARCH DESIGN AND METHODS

Cell Culture
Cell culture experiments were performed on immortal hypothalamic GT1-7 cells cultured in high-glucose (4.5 mg/dL) DMEM, 10% FBS, and 1% penicillin-streptomycin. Cells were treated with 3.65 mmol/L α-klotho (R&D Systems) (10,11,28), treated with 100 ng/mL FGF23 (R&D Systems) (28), and/or pretreated with 10 nmol/L FGFR1 antagonist PD173074 (Fisher Scientific) (29) or 50 nmol/L PI3K inhibitor wortmannin (Fisher Scientific) (25). All experiments used vehicle-treated cells as controls.

Experimental Animals
C57BL/6 and B6.Tg(NPY-hrGFP)1Lowl/J (NPY-GFP reporter) mice were cared for in accordance with the National Institutes of Health *Guide for the Care and Use of Laboratory Animals*, and experimental protocols were approved by Institutional Animal Care and Use Committees of East Carolina University. Mice were housed at 20–22°C with a 12-h light-dark cycle.

High-Fat Diet–Induced Obesity
The 6-week-old male C57BL/6 mice were given ad libitum access to a high-fat diet with a kilocalorie composition of 58%, 25%, and 17% of fat, carbohydrate, and protein, respectively, for 10 weeks (D12331; Research Diets, New Brunswick, NJ) before undergoing intracerebroventricular (ICV) cannulation.

ICV Cannulation
Prior to the procedure, mice were given oral analgesic meloxicam and anesthetized with intraperitoneal (i.p.) injection of ketamine and xylazine. Mice were placed on a stereotaxic device, and a midline incision was made on the head. A hole was drilled (1.0 mm lateral, -0.5 mm posterior, 2.5 mm deep to the bregma), and a cannula was placed into the lateral ventricle (Supplementary Fig. 1). Another hole was drilled, and a screw was placed approximately at the ipsilateral lambdoid structure to aid in supporting the cannula in the skull with 3M carboxylate dental cement. Mice recovered for 14 days before immunohistochemical experiments and 7 days before all other experiments. All ICV treatments were administered via Hamilton syringe as 2.0 μL between 6:30 and 7:30 P.M.

The 12-Day ICV Injection Timeline
In high-fat diet–induced obesity (DIO) mice, central administration of either 2.0 μg recombinant α-klotho (R&D

Systems) alone, 25.0 μg PD173074 alone, 25.0 μg PD173074 10 min before 2.0 μg α-klotho (20), or vehicle was performed daily. On day 7, glucose tolerance tests (GTTs) or insulin tolerance tests (ITTs) were performed, and on day 12, a body composition analysis was performed using EchoMRI (Echo Medical Systems, Houston, TX). Mice were then euthanized, and tissues were collected. Food intake and body weight data were analyzed from the first 7 days to prevent confounding effects from additional assays.

Single ICV Injection Timeline
In DIO mice, ICV administration of either 2.0 μg recombinant α-klotho (R&D Systems), 10 ng wortmannin, 10 ng wortmannin 1 h before 2.0 μg α-klotho (30), or vehicle was performed the night before a GTT or ITT. Food intake was measured for 4 days after the injection.

Streptozotocin-Induced Diabetes
The 8- to 9-week-old chow-fed male mice underwent ICV cannulation before receiving 3 days i.p. injection of 100 mg/kg streptozotocin (STZ). The dose was determined by pilot studies yielding consistently elevated fed glucose levels between 250 and 600 mg/dL (Supplementary Fig. 2A). At 7 days after STZ injection, mice received 7 days ICV treatment with either 2.0 μg recombinant α-klotho ($n = 10$) or vehicle ($n = 9$). Food intake, body weight, and fed glucose levels were monitored daily. To identify the effects of α-klotho treatment on glucose levels independent from food intake, a pair-fed experiment was performed using the same protocols, and on day 7, fasting glucose levels were measured ($n = 8–9$/group).

Central α-Klotho Inhibition via ICV Anti–α-Klotho Antibody
The 9-week-old male, chow-fed mice were ICV treated with 1.0 μg anti–α-klotho (ab-α-klotho) (R&D Systems) or vehicle ($n = 8$/group). Treatments were performed on the evening of day 1 and morning of day 2, while subsequent treatments were performed between 6:30 and 7:30 P.M. for 7 days. GTTs were performed on day 3, and on day 7, mice were euthanized, followed by tissue collection for further assays.

Food Intake Measurements
Food intake was measured daily by weighing food (8–9 g) and subtracting from the total food. Bedding was inspected thoroughly for residual bits of food, which were included in measurements. On day 4 in one cohort of DIO mice, food was removed from cages during the light phase and replenished at the beginning of the dark phase (7:30 P.M.). Food intake was measured at 0.5, 1, 1.5, 2, 3, 4, 8, 14, and 24 h after food reintroduction.

GTTs and ITTs
For GTTs, 20% glucose solution (1.0 g/kg body weight) was i.p. injected after an overnight fast, and for ITTs, 0.6 units/kg insulin were i.p. injected after a 4-h fast. Tail blood

samples were collected 15, 30, 60, 90, and 120 min after injections for analysis using a glucose meter (ReliOn Prime Blood Glucose Monitoring System; ARKRAY Inc., Kyoto, Japan). Serum was isolated from clotted blood spun at 4°C and 2,000g for 30 min. Insulin levels were quantified using an insulin ELISA kit (Crystal Chem).

Insulin-Stimulated Signaling
On day 12 of ICV treatment, a weight-matched cohort of DIO mice was i.p. injected with 10 units/kg insulin or saline. At 7 min after the injection, hypothalamus, epididymal adipose tissue (eWAT), liver, and hindlimb skeletal muscle were flash frozen for future Western blot analysis.

Immunohistochemistry
For immunofluorescent analysis, mice were intracardially perfused with PBS followed by 10% formalin before immunohistochemistry was performed as described previously (31). Briefly, brains were sliced into 20-μm coronal sections using a freezing microtome (VT1000 S; Leica, Wetzlar, Germany) and incubated overnight in antibody to phosphorylated ERK (1:500; Cell Signaling Technology, Danvers, MA) or cFOS (1:500; Santa Cruz Biotechnology, Santa Cruz, CA), followed by incubation with Alexa-fluorophore secondary antibody for 2 h. Stains were photographed using an optical microscope (DM6000; Leica), followed by blind analysis using ImageJ. At least three anatomically matched images per mouse were quantified.

Western Blot
Western blot was performed as described previously (31). Briefly, equal protein samples were loaded into a 4–20% HCL gel, transferred to a nitrocellulose membrane, and incubated overnight in 1:500–1:1,000 antibody dilutions in 5% milk with Tris-buffered saline with Tween for phosphorylated (p)AT^{ser473}, total AKT, pFOXO1^{ser256}, total FOXO1, pERK$^{thr202/thr204}$ (Cell Signaling Technology), pIR^{tyr972} (Invitrogen), and total ERK (Santa Cruz). Image J software was used to quantify mean intensity of equal-area sections representing each sample.

Quantitative PCR
Cell and tissue RNA was extracted by Trizol (Thermo Fisher Scientific, Waltham, MA). The expressions of specific mRNA were analyzed using quantitative real-time PCR (RT-qPCR) (Power SYBR Green PCR Master Mix; Applied Biosystems, Foster City, CA). Reactions were performed in triplicate for each sample, while GAPDH was used as a reference gene for normalization.

Patch Clamp Electrophysiology
We conducted cell-attached voltage clamp recordings of NPY/AgRP neurons as described previously (32,33). Briefly, mice were deeply anesthetized by isoflurane followed by intracardial perfusion with chilled N-methyl-D-glucamine solution and sliced into 200- to 300-μm sections. Slices recovered for an hour in HEPES recovery solution, and recordings were conducted in a normal artificial cerebrospinal fluid (aCSF) bath. For whole cell recordings, gigaohm seals were obtained, and the cells were broken into using negative pressure. Data were sampled at 10 kHz. Current clamp recordings were stabilized for repeated firing under the baseline condition. Equivalent length periods (0.5–5 min) were set within each recording during perfusion of aCSF or α-klotho (3.65 mmol/L). Firing rate (Hz) was calculated by dividing the number of events by the number of seconds. Bath application of terodotoxin (TTX) (1.0 μmol/L) prior to α-klotho treatment was used to determine action potential–independent effects on membrane potential. Voltage clamp whole cell recordings were conducted at a −70 mV holding potential and a high KCl intracellular solution (130 mmol/L KCl, 5 mmol/L CaCl$_2$, 10 mmol/L EGTA, 10 mmol/L HEPES, 2 mmol/L magnesium adenosine triphosphate, 0.5 mmol/L sodium guanosine triphosphate, and 5 mmol/L phosphocreatine) was used. For voltage clamp recordings of miniature inhibitory postsynaptic currents (mIPSCs), glutamatergic blockade was induced using NMDA receptor blocker AP5 (50 μmol/L) and AMPA receptor blocker cyanquixaline (10 nmol/L), followed by α-klotho administration, and then currents were abolished with picrotoxin (100 μmol/L) (34).

Statistical Analysis
Unpaired t tests were used for in vivo mouse experiments to compare differences between groups in food intake, body weight, and body composition. To compare pre-post within-group changes over the course of the experiment, paired t tests were performed. To compare differences at GTT or ITT time points, two-way ANOVA with repeated measures for time and Bonferroni corrections for multiple comparisons were used. Unpaired t tests or one-way ANOVA with Tukey correction for multiple comparisons were used in cell culture experiments when appropriate. Paired t tests or repeated-measures ANOVA with Tukey correction for multiple comparisons was used in patch clamp electrophysiology experiments when appropriate. All analyses were performed using GraphPad Prism statistics software, and a P value <0.05 was considered statistically significant.

Data and Availability Statement
The data sets generated during the current study are available from the corresponding author on reasonable request.

RESULTS

Seven Days of Central Administration of α-Klotho Results in Weight Loss, Suppressed Food Intake, and Improved Glucose Regulation in DIO Mice
A 7-day ICV α-klotho treatment in DIO mice significantly reduced body weight (4.9%) compared with vehicle-treated controls (Fig. 1A and B). These changes were, at least in part, due to decreased food intake both daily (14.8%) and after a daytime food restriction (11.4%) (Fig. 1E–H). ICV α-klotho treatment also improved glucose clearance and

insulin release during a GTT, as well as insulin sensitivity during an ITT (Fig. 1I–N).

A Single ICV α-Klotho Injection Improves Glucose Clearance and Suppresses Food Intake in DIO Mice

To determine if the effects of central α-klotho on glucose metabolism were independent from changes in body weight, a single ICV α-klotho injection was performed in DIO mice the night before a GTT or ITT. Acute ICV α-klotho treatment improved glucose clearance during a GTT (Fig. 2A–C) and even decreased food intake the following day (Fig. 2D). Interestingly, acute ICV α-klotho treatment had no effects on insulin sensitivity (Fig. 2E–H). These data suggest central α-klotho regulates glucose metabolism independent from changes in body weight and insulin sensitivity. Supporting this hypothesis, 12 days of ICV α-klotho had no effects on insulin-stimulated signaling in hypothalamus, skeletal muscle, eWAT, or liver in weight-matched DIO mice (Supplementary Fig. 3).

To begin to investigate alternative peripheral mechanisms through which central α-klotho improves glucose regulation, basal hepatic gene expression was analyzed. Hepatic PEPCK mRNA was significantly reduced (0.75-fold reduction) in DIO mice treated with α-klotho for 12 days, suggesting attenuated hepatic gluconeogenesis, despite no changes in pyruvate kinase, glucose-6-phsophatase, or glucokinase. α-Klotho–treated mice also had reduced
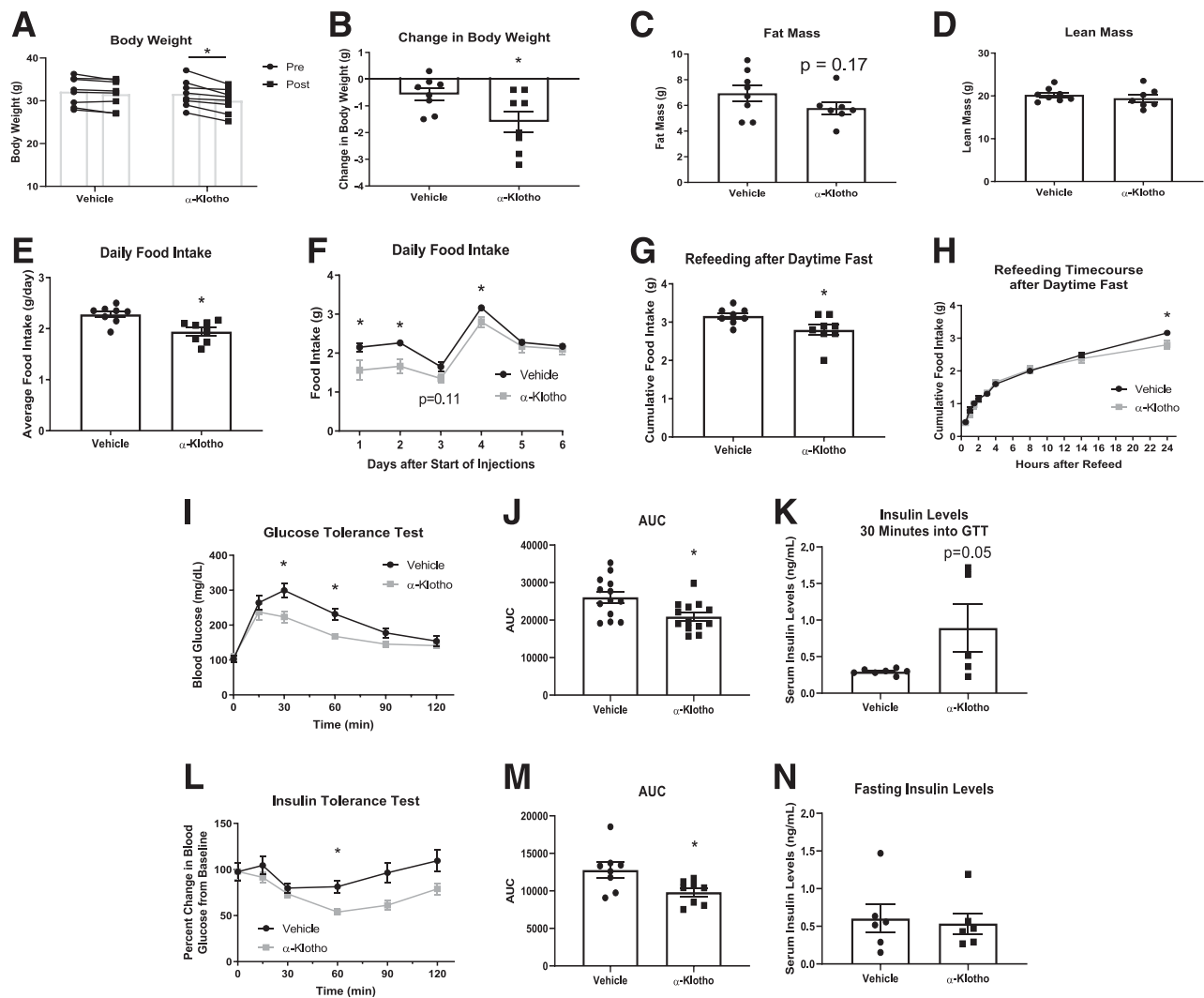

Figure 1—Seven days of central administration of α-klotho results in weight loss, suppressed food intake, and improved glucose regulation in DIO mice. A: Body weight. B: Changes in body weight. C: Fat mass. D: Lean mass. E: Average daily food intake. F: Timeline of daily food intake. G: Cumulative food intake after a daytime food restriction. H: Timeline of food intake after a daytime food restriction. I: Blood glucose levels during a GTT. J: Area under the curve (AUC) of the GTT. K: Serum insulin levels 30 min into the GTT. L: Blood glucose during an ITT. M: AUC of the ITT. N: Fasting serum insulin. A–N: In 17- to 18-week-old male DIO mice after 7 days ICV α-klotho or vehicle injections (n = 8–13/group). Data represented as mean ± SEM. *P < 0.05 vs. ICV control.
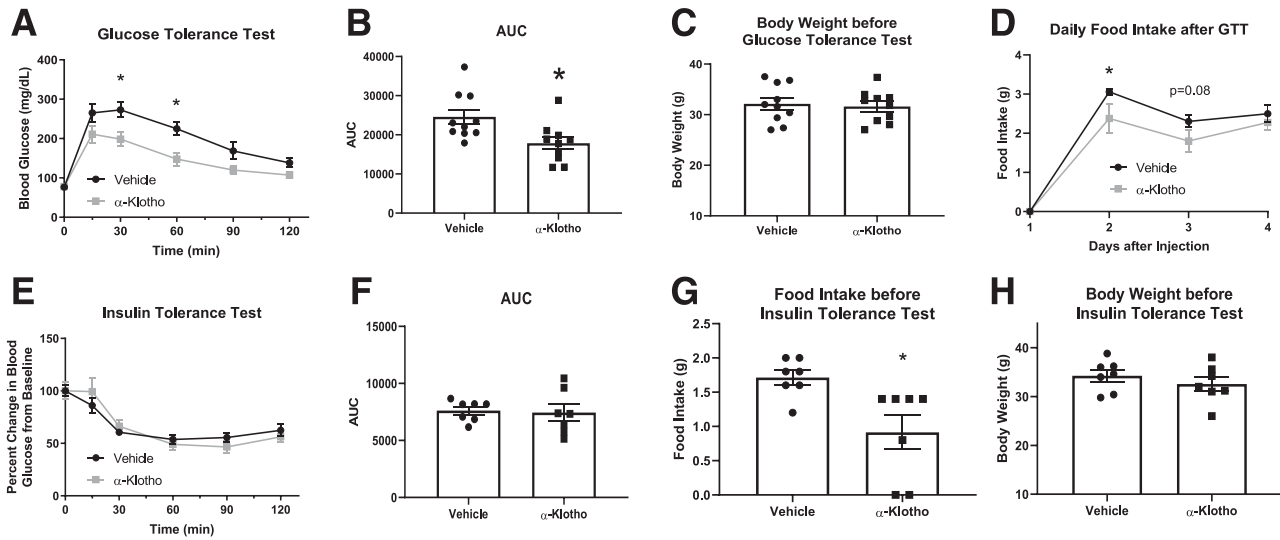
1 Day Treatment in DIO Mice

Figure 2—Acute central administration of α-klotho improves glucose clearance and suppresses food intake independent of body weight in DIO mice. A: Blood glucose during a GTT. B: Area under the curve (AUC) of the GTT. C: Body weight before the GTT. D: Daily food intake (including overnight fast before GTT on day 1). E: Blood glucose during an ITT. F: AUC of the ITT. G: Food intake the night before the ITT. H: Body weight before the ITT. A–H: In 17- to 18-week-old male DIO mice after a single ICV α-klotho or vehicle injection (n = 7–10/group). Data represented as mean ± SEM. *P < 0.05 vs. ICV control.

hepatic lipid accumulation and upregulated ACC1 and ACC2 mRNA (Supplementary Fig. 4).

Seven Days of Central α-Klotho Administration Attenuates the Progression of Diabetes in STZ-Treated Mice

The therapeutic potential of α-klotho was also investigated in a model of type 1 diabetes induced by STZ treatment. Similar to DIO mice, ICV α-klotho decreased body weight (5.3%), suppressed food intake (27.8%), and attenuated hyperglycemia (20.2% reduction in fed glucose levels) in STZ-treated mice compared with vehicle-treated controls (Fig. 3A–G). Even in pair-fed STZ-treated mice, ICV α-klotho attenuated hyperglycemia and trended to improve fasting glucose levels (Fig. 3K–M). These data further demonstrate glucoregulatory and anorexic action of central α-klotho in both type 1 and type 2 diabetes models.
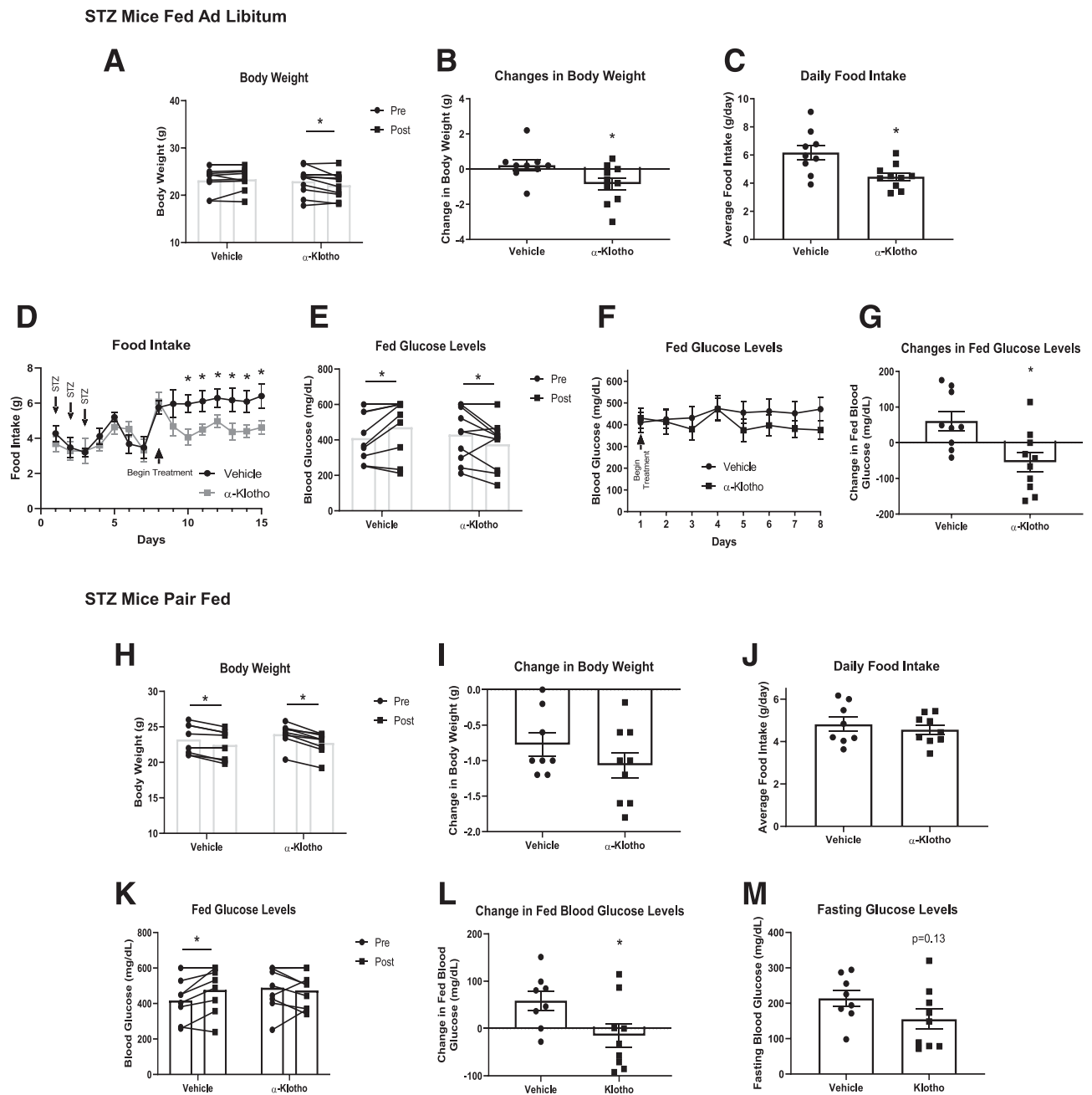
Central α-Klotho Inhibition Impairs Glucose Tolerance

To determine the effects of central α-klotho inhibition on energy and glucose homeostasis, we performed central administration of ab-α-klotho antibody. A 2-day ab-α-klotho treatment significantly impaired glucose tolerance compared with vehicle-treated controls despite similar body weights (Fig. 4A–C). There were no differences in liver PEPCK or glucose-6-phsophatase. However, gene expression of glucokinase and pyruvate kinase trended to be lower in ab-α-klotho mice (P = 0.14 and 0.15, respectively) (Supplementary Fig. 5D). Surprisingly, 7 days of ab-α-klotho significantly decreased body weight

with no changes in food intake (Fig. 4D–G). Taken together with ICV α-klotho experiments, these data suggest a distinct glucoregulatory role of central α-klotho independent of body weight and food intake.

α-Klotho Suppresses NPY/AgRP Neuron Activity, at Least in Part, by Enhancing mIPSCs

We next aimed to investigate the effects of α-klotho on NPY/AgRP neurons considering their critical role in energy homeostasis. A single ICV α-klotho injection in NPY-GFP reporter mice before an overnight fast significantly reduced cFOS colocalization with NPY/AgRP neurons by 49.0% (Fig. 5A–C). Furthermore, electrophysiological recordings revealed α-klotho treatment decreases NPY/AgRP neuron firing rate and membrane potential (0.79 vs. 0.22 Hz and −52.7 vs. −57.8 mV, respectively) (Fig. 5D–F).

To determine if α-klotho's suppressive effects on NPY/AgRP neurons are due to pre- or postsynaptic events, brain slices were pretreated with TTX (1.0 μmol/L) to block action potentials. In the presence of TTX, α-klotho still decreased membrane potential (−53.4 vs. −58.4 mV), suggesting postsynaptic action of α-klotho on NPY/AgRP neurons (Fig. 5G and H). We also observed α-klotho to increase the magnitude, but not the frequency, of mIPSCs in NPY/AgRP neurons under glutamatergic blockade (25.9 vs. 34.4 pA) (Fig. 5I–M), indicating α-klotho is directly antagonizing NPY/AgRP neurons by modulating receptor availability or intracellular signals (35). Overall, these experiments illustrate that α-klotho directly suppresses NPY/AgRP neuron activity by, at least in part, increasing receptor-mediated inhibitory signals.

STZ Mice Fed Ad Libitum

STZ Mice Pair Fed

Figure 3—Seven days of central α-klotho administration attenuates the progression of diabetes in STZ-treated mice. *A*: Body weight. *B*: Changes in body weight. *C*: Average daily food intake. *D*: Timeline of food intake. *E*: Fed blood glucose levels. *F*: Timeline of fed blood glucose. *G*: Change in fed blood glucose levels. *A*–*G*: In 9- to 10-week-old, STZ-treated, ad libitum fed mice after 7 days ICV α-klotho or vehicle injections (*n* = 9–10/group). *H*: Body weight. *I*: Changes in body weight. *J*: Average daily food intake. *K*: Fed blood glucose levels. *L*: Change in fed blood glucose levels. *M*: Fasting blood glucose levels. *H*–*M*: In pair-fed, STZ-treated mice (*n* = 8–9/group). Data represented as mean ± SEM. *$P < 0.05$ vs. ICV control.

α-Klotho Induces Cell Signaling, Alters Gene Expression, and Decreases NPY/AgRP Neuron Activity via FGFRs

To investigate the potential of α-klotho to alter cell signaling and gene expression in the hypothalamus, we first used the GT1-7 immortal hypothalamic cell line (36). A 30-min α-klotho treatment increased phosphorylation of ERK$^{thr202/tyr204}$, AKT^{ser473}, and FOXO1^{ser256}

(Supplementary Fig. 6*A*). Additionally, α-klotho treatment during both overnight and 2 h of serum starvation significantly reduced AgRP mRNA (by 28.5% and 30.3%, respectively), suggesting hormonal action of α-klotho in GT1-7 cells (Supplementary Fig. 6*C*). To investigate if α-klotho has hormonal action in the hypothalamus in vivo, we performed acute ICV α-klotho administration in healthy, fed mice and observed elevated phosphorylated
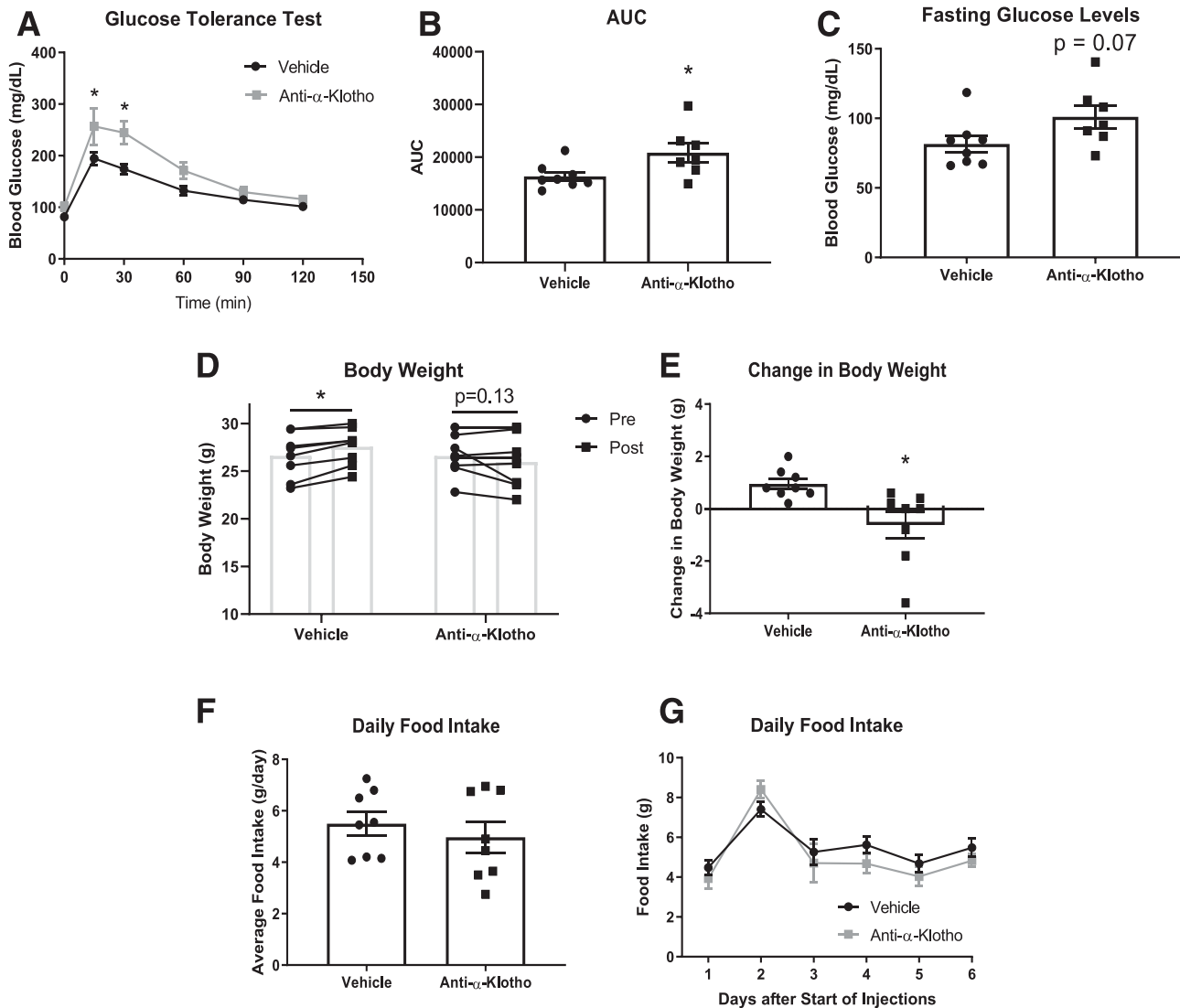
Figure 4—Central α-klotho inhibition impairs glucose tolerance. *A*: Blood glucose levels during a GTT. *B*: Area under the curve (AUC) of the GTT. *C*: Fasting glucose levels. *D*: Body weight. *E*: Changes in body weight. *F*: Daily food intake. *G*: Timeline of food intake. *A–G*: In 9-week-old chow-fed male mice treated with ab-α-klotho antibody compared with vehicle-treated controls (*n* = 8/group). Data represented as mean ± SEM. *P < 0.05 vs. ICV control.

ERK after 90 min in the ARC compared with vehicle-treated controls (Supplementary Fig. 6*B*).

Previous studies demonstrate the importance of α-klotho as a scaffolding protein increasing the affinity of FGF23 to FGFR1 (26,27). In hypothalamic GT1-7 cells, 30-min FGF23 (100 ng/mL) treatment had no effects on phosphorylated ERK or AKT (Fig. 6*A–C*), while cotreatment with FGF23 and α-klotho had no synergistic effect compared with α-klotho alone. This suggests, at least in hypothalamic GT1-7 cells, α-klotho is independent of exogenous FGF23-mediated signaling. When cells were pretreated with FGFR1 inhibitor PD173074 (10 nmol/L), α-klotho–mediated cell signaling and suppression of AgRP mRNA were abolished (Fig. 6*A–D*), indicating hypothalamic α-klotho action is dependent on FGFR1 activity. Moreover, immunofluorescent staining of cFOS

revealed that ICV pretreatment with PD173074 also inhibited the ability of α-klotho to decrease NPY/AgRP neuron activity in vivo (Fig. 6*E–G*).

PI3K is a downstream mediator of FGFR1 and is also an important negative regulator of NPY/AgRP neurons (25,37). PI3K inhibition using wortmannin (50 nmol/L) also eliminated α-klotho's ability to suppress AgRP gene expression (Fig. 6*D*). Taken together, these data demonstrate the importance of FGFR1/PI3K signaling in hypothalamic α-klotho function.

Seven Days of Central α-Klotho Treatment Suppresses Food Intake and Reduces Body Weight via FGFR and PI3K Signaling in DIO Mice
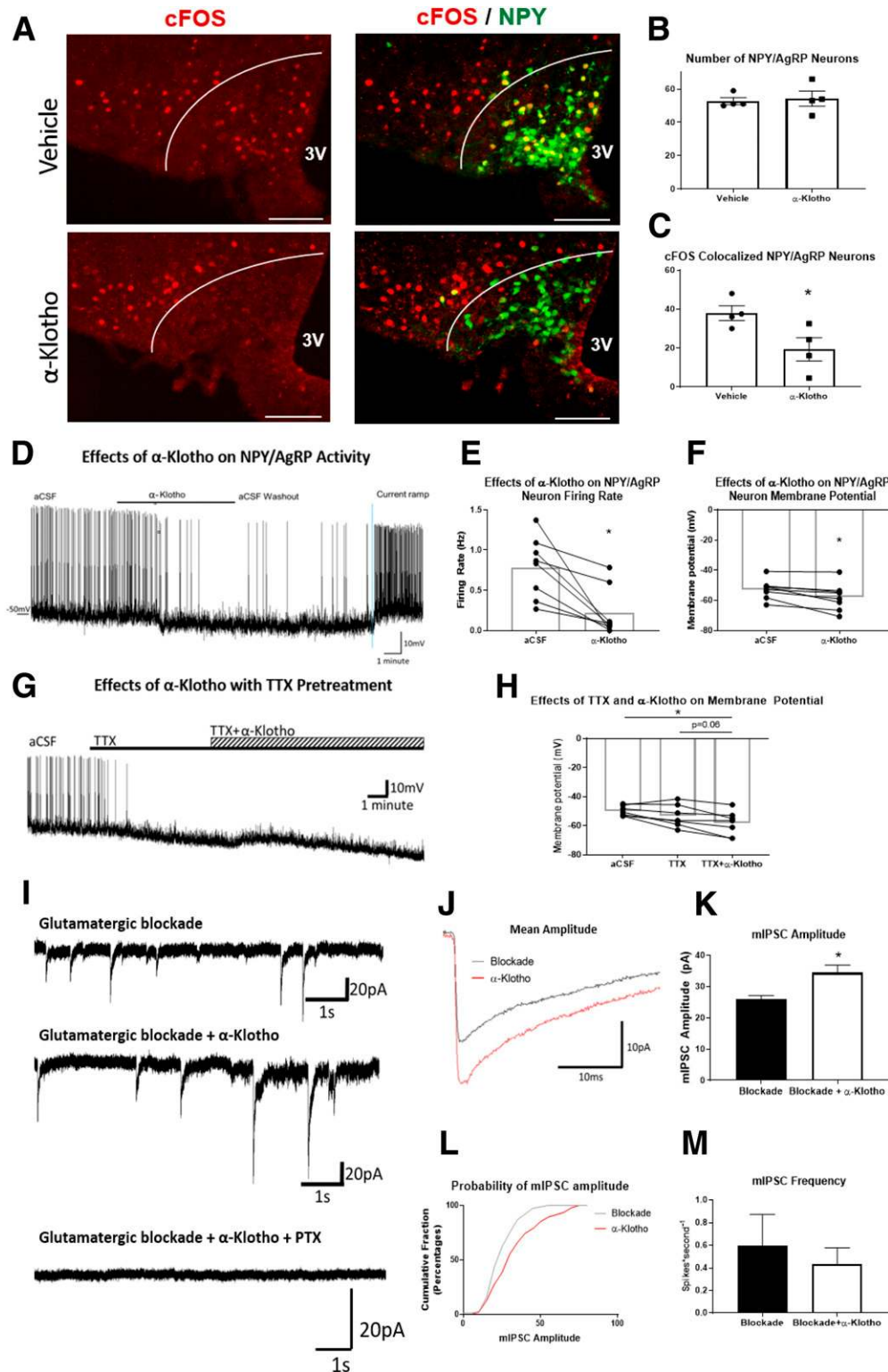To determine if the therapeutic effects of α-klotho in DIO mice were dependent on FGFRs, we centrally injected

Figure 5—α-Klotho suppresses NPY/AgRP neuron activity, at least in part, by enhancing mIPSCs. *A*: Representative image of cFOS (red) colocalization with NPY/AgRP (green). *B*: Number of NPY neurons. *C*: Number of NPY neurons with cFOS colocalization in the ARC. *A–C*: Mice ICV treated with 2.0 μL α-klotho or vehicle before an overnight fast (*n* = 4 mice/group). *D–F*: Representative cell-attached recording of an NPY/AgRP neuron (*D*), calculated firing rate (Hz) (*E*), and membrane potential (mV) (*F*) during α-klotho administration (*n* = 8 neurons from four male mice). *G* and *H*: Representative current clamp trace of an NPY/AgRP neuron (*G*) and mean membrane potential (*H*) induced by TTX or TTX and α-klotho. *I*: Representative whole cell recording tracers with α-klotho, glutamatergic blockade, and GABA-A receptor antagonist picrotoxin. *J–M*: Mean amplitude (*J* and *K*), differences in cumulative probability of mIPSC amplitude (*L*), and mean frequency (*M*) of IPSCs under glutamatergic blockade with and without α-klotho treatment (*n* = 5 neurons from three male mice). Data represented as mean ± SEM. *$P < 0.05$ vs. aCSF.

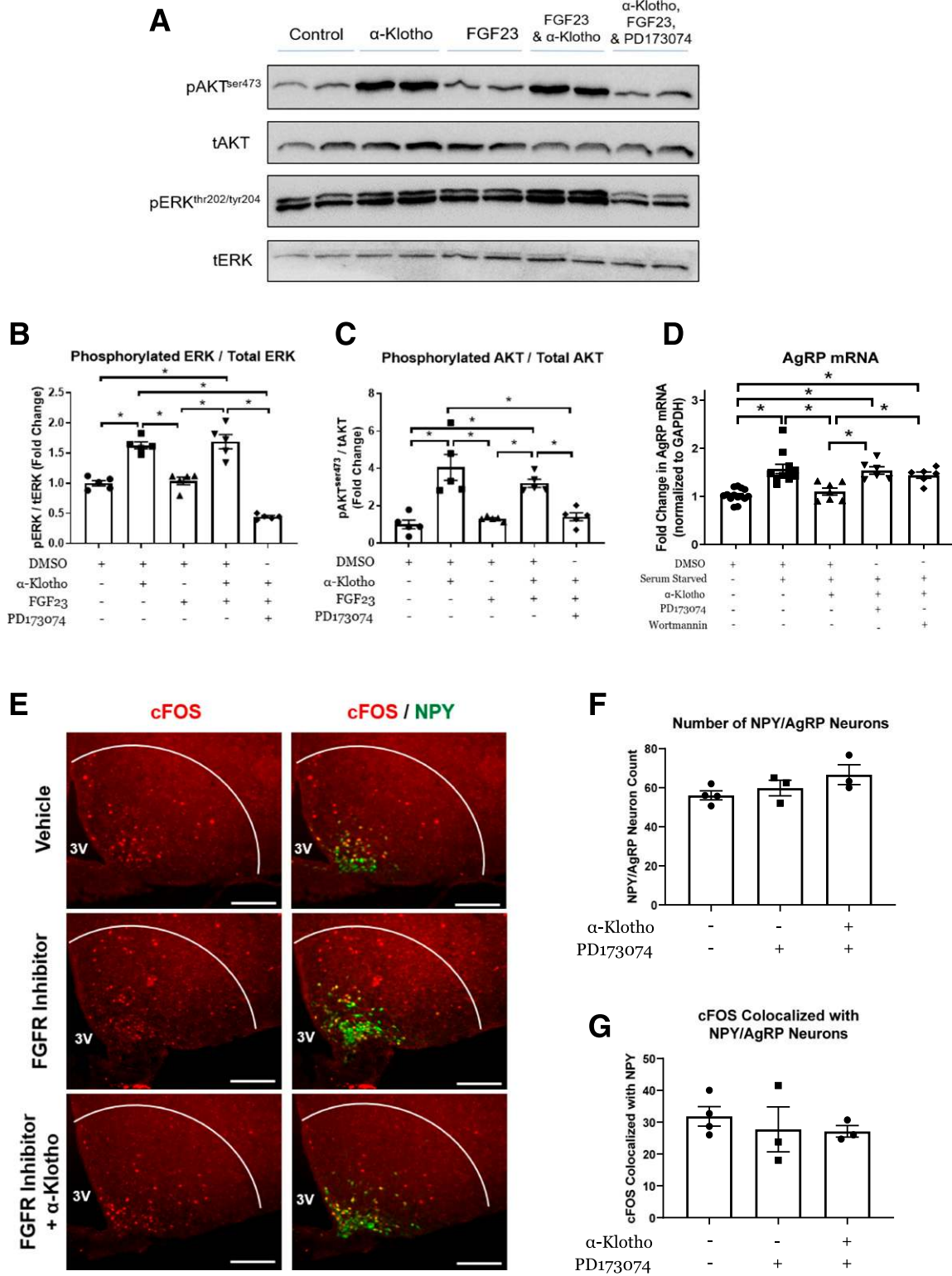**Figure 6**—α-Klotho–mediated cell signaling and regulation of NPY/AgRP neurons in the hypothalamus is dependent on FGFRs. *A*: Representative Western blot image. *B*: Phosphorylation of ERK. *C*: Phosphorylation of AKT. *D*: AgRP mRNA expression. *A–C*: In GT1-7 cells treated with α-klotho, FGF23, PD173074, and/or wortmannin (*n* = 5–10/group). *E*: Representative image of cFOS (red) colocalization with NPY/AgRP neurons (green). *F*: Number of NPY neurons. *G*: Number of NPY neurons colocalized with cFOS. *D–G*: In the ARC of the hypothalamus of mice ICV treated with vehicle, FGFR inhibitor with vehicle, or FGFR inhibitor with α-klotho before an overnight fast (*n* = 3 mice/group). Data represented as mean ± SEM. *P* < 0.05 vs. controls. tAkt, total Akt; tERK, total ERK.

PD173074 to inhibit endogenous FGFR function. Mice receiving α-klotho treatment alone experienced significantly decreased food intake and body weight compared with all groups (Fig. 7A–D), while PD173074 treatment alone induced weight gain (Fig. 7A and B). PD173074 treatment blunted α-klotho–mediated reductions in food intake and body weight, suggesting the effects of central α-klotho on energy balance are mediated by FGFR signaling. Surprisingly, both α-klotho with an FGFR inhibitor and α-klotho alone groups experienced improved glucose clearance compared with vehicle-treated controls (Fig. 7E and F), suggesting FGFRs may not be involved in central α-klotho–mediated glucose regulation.

Similar to FGFR antagonism, central inhibition of PI3K abolished α-klotho's ability to suppress food intake and improve glucose clearance (Fig. 8). These data indicate that PI3K is critical to α-klotho–mediated regulation of food intake and glucose metabolism. Overall, coupled with in vitro cell signaling experiments, these data demonstrate a novel α-klotho/FGFR/PI3K mechanism in the central regulation of metabolism.

DISCUSSION

To our knowledge, this is the first study to provide evidence that α-klotho functions as a hypothalamic hormonal agent. ICV α-klotho administration improved glucose regulation, suppressed food intake, and reduced body
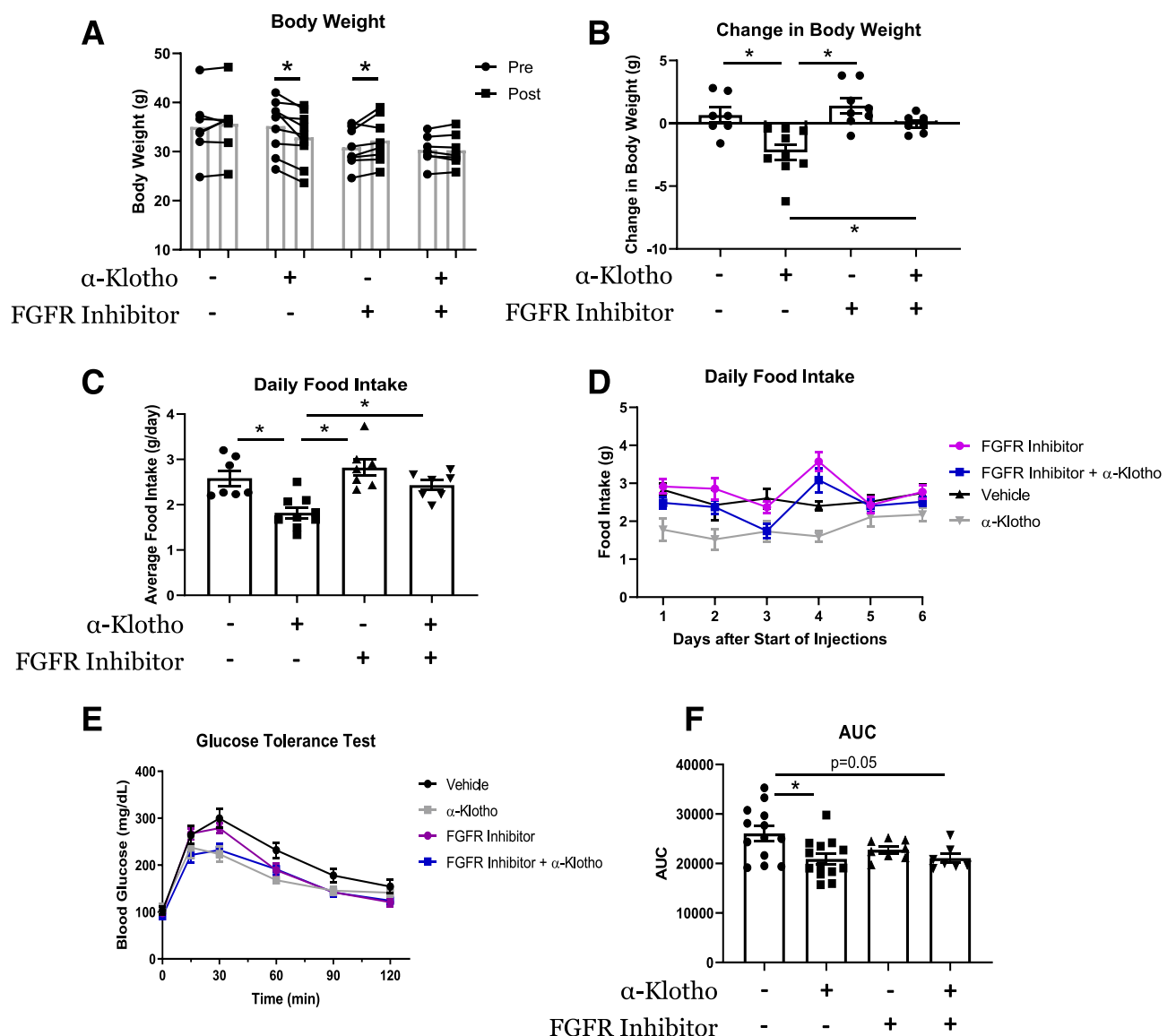

Figure 7—Central inhibition of FGFR1 blunts the therapeutic effects of 7 days α-klotho in DIO mice. A: Body weight. B: Changes in body weight. C: Average daily food intake. D: Timeline of food intake. E: Blood glucose levels during GTT. F: Area under the curve (AUC). A–F: In DIO mice receiving 7 days ICV injection with vehicle, α-klotho, FGFR inhibitor, or inhibitor with α-klotho ($n = 7$–11/group). Data represented as mean $\pm$ SEM. *$P < 0.05$ vs. ICV vehicle.
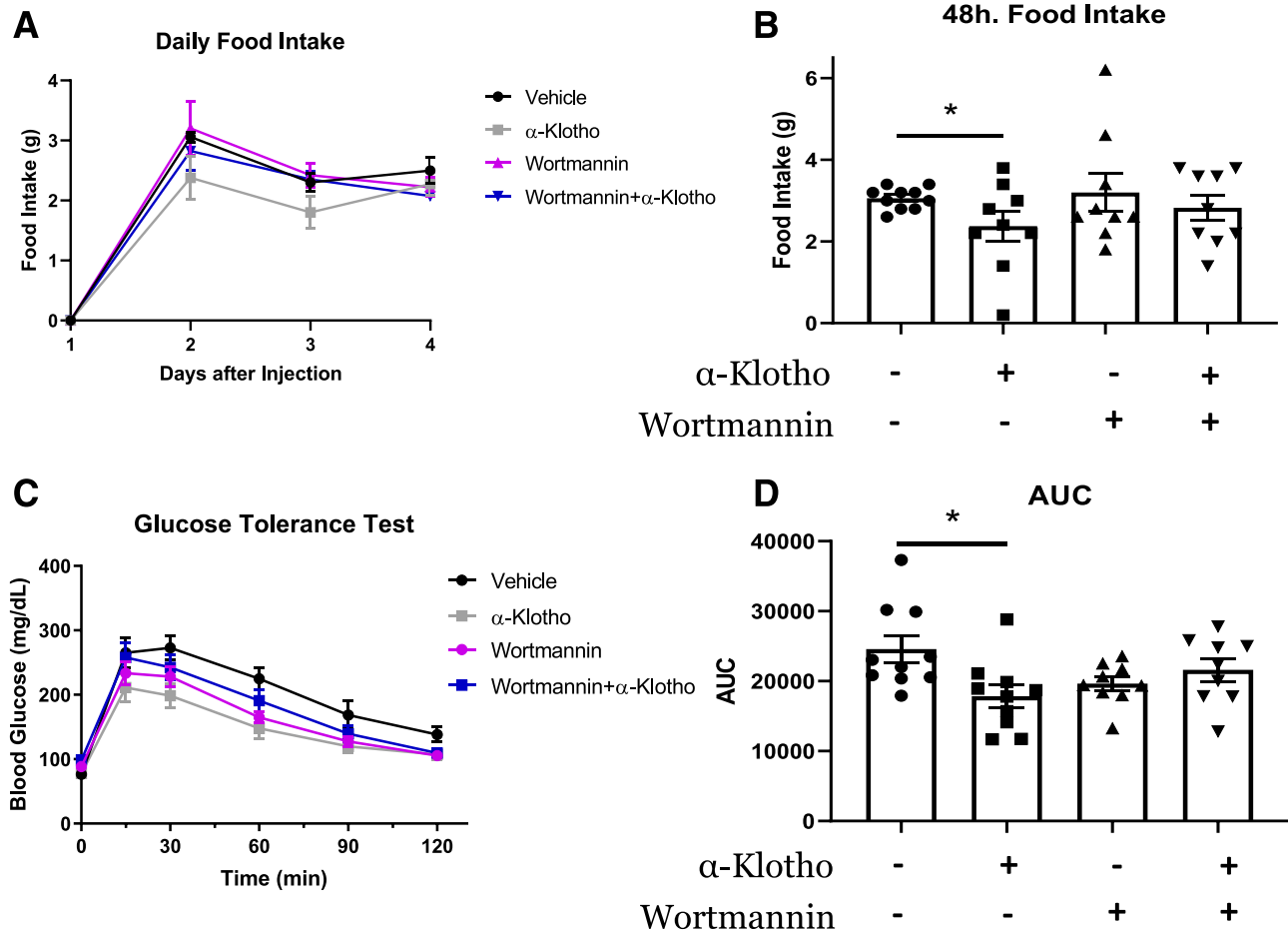
Figure 8—Central inhibition of PI3K negates the therapeutic effects of a single α-klotho injection in DIO mice. *A*: Timeline of food intake (including overnight fast before GTT on day 1). *B*: Average 48-h food intake. *C*: Blood glucose during a GTT. *D*: Area under the curve (AUC) of the GTT. *A*–*D*: In DIO mice receiving a single injection with vehicle, α-klotho, wortmannin, or wortmannin with α-klotho (n = 9–10/group). Data represented as mean ± SEM. *P < 0.05.

weight in mouse models of type 1 and 2 diabetes, illustrating the therapeutic potential of central α-klotho in metabolic disease states. Although deeper investigation is required to identify the direct connection between central α-klotho activity and peripheral glucose metabolism, the current study determined that the glucose-lowering effects of α-klotho are independent from insulin sensitivity but, rather, are mediated by augmented insulin secretion during a glucose challenge. However, STZ experiments revealed that some of the glucoregulatory actions of α-klotho are independent of insulin altogether. Basal hepatic PEPCK mRNA was decreased in α-klotho-treated DIO mice, suggesting decreased hepatic glucose output may be an alternative mechanism.

The central and peripheral pools of α-klotho have distinct, independent functions due to α-klotho's inability to cross the blood-brain barrier (9). While recent publications have demonstrated metabolic roles of α-klotho in the blood, including long-term α-klotho injection improving adiposity in DIO mice (6) and ameliorating diabetic cardiomyopathies in STZ-treated mice (38), the current study

identifies distinct differences between central and peripheral α-klotho–mediated metabolic regulation. For example, α-klotho's effects on food intake and glucose metabolism seem to be mainly via central mechanisms, while peripherally circulating α-klotho regulates gene expression to promote lipid oxidation and energy expenditure (6,38). Notably, whole-body α-klotho knockout and knockdown models have been previously utilized to investigate α-klotho's functions (1,7), but these approaches do not distinguish between peripheral and central α-klotho function.

ICV ab-α-klotho was used in this study as a novel approach specifically impairing central α-klotho signaling, and as expected, ab-α-klotho treatment impaired glucose clearance. Although central α-klotho concentrations have yet to be quantified in patients with diabetes, past studies show blood α-klotho concentrations to be decreased in some populations with diabetes (8,39). Thus, our data connecting central α-klotho impairment and disordered glucose regulation may provide new insight into the pathophysiology of metabolic disorders.

Contrary to our hypotheses, central α-klotho inhibition resulted in decreased body weight with no differences in food intake. α-Klotho knockout mice also experience weight loss, primarily due to atrophy of metabolically active organs, resulting in premature death (1,7). These findings highlight the complicated and diverse metabolic functions of α-klotho. For example, while evidence from the current study and past literature describes α-klotho as an antidiabetic agent (3–6,38), overexpression of α-klotho has been shown to elicit insulin resistance (1). Notably, α-klotho–overexpressing mice do not experience hyperglycemia, adiposity, or hyperphagia associated with clinical insulin resistance (1). Moreover, α-klotho is an important negative modulator of insulin and IGF-I signaling to regulate apoptosis and ROS buffering (10,11). The many complex physiological roles of α-klotho may explain the unexpected results in response to central α-klotho inhibition.

The current study identified central α-klotho as a novel antagonist of NPY/AgRP neurons. Considering NPY/AgRP neuron overactivity is associated with disordered feeding, body weight, and glucose regulation (13,40), our data provides encouraging evidence of α-klotho as a potential therapeutic target in metabolic disease prevention. At the present, it is unclear if NPY/AgRP neurons are the primary mediators of central α-klotho's regulation of metabolism, underscoring the importance of further investigation into the specific neuronal effectors and cell signaling involved. However, the observed ICV α-klotho phenotype has many similarities to the previously described effects of NPY/AgRP neuron inhibition, including suppressed food intake, reduced body weight, improved glucose clearance and insulin release, and decreased hepatic gluconeogenic gene expression (13,15–17,41,42).

Similar to findings in studies using hippocampal and oligodendrocyte progenitor cells (10,11,28), α-klotho induced phosphorylation of ERK$^{thr202/tyr204}$, AKT^{ser473}, and FOXO1^{ser256} in hypothalamic GT1-7 cells—all of which are established signaling molecules involved in downregulating NPY/AgRP gene transcription and activity (18,43). Furthermore, the observed ICV α-klotho phenotype resembles FGFR activation, which also results in suppressed food intake, improved glucose regulation, attenuated NPY/AgRP neuron activity, and decreased liver gluconeogenic gene expression (20–24). α-Klotho serves as a nonenzymatic scaffold to increase FGF23 affinity to FGFR1 (27). Thus, we investigated the potential importance of a hypothalamic α-klotho–FGFR1 signaling mechanism. Similar to previous studies in hippocampal cells, our results show that hypothalamic α-klotho–mediated signaling and AgRP mRNA regulation in GT1-7 cells were abolished with pretreatment with FGFR1 antagonist PD173074 (28). Additional experiments determined that PI3K signaling, a downstream mediator of FGFR1 (37) and potent regulator of NPY/AgRP neurons (25), was also required for α-klotho–mediated AgRP mRNA suppression. Future studies should further investigate the possible involvement of a novel α-klotho–FGFR1–PI3K axis in the homeostatic modulation of NPY/AgRP neurons.

We further investigated the involvement of FGFR/PI3K signaling to central α-klotho–mediated regulation of metabolism. Central FGFR or PI3K inhibition blunted ICV α-klotho's effects on food intake and body weight, while only PI3K inhibition affected α-klotho–mediated glucose regulation. Overall, these data support the hypothesis that central FGFR-PI3K signaling is critical to α-klotho–mediated regulation of metabolism. However, studies investigating the function of central FGFRs in metabolism yield mixed results depending on animal model and experimental approach. ICV PD173074 (FGFR inhibitor) impairs glucose clearance in healthy rats, but it is described as stress related (23,44). ICV PD173074 in DIO mice elicits no phenotype (21,24). Furthermore, antibody-mediated inhibition of FGFR1 in rodents and monkeys increases energy expenditure, decreases food intake, and reduces body weight, while genetic deletion of FGFR1 in NPY/AgRP neurons also results in no metabolic phenotype (45–47). Additionally, the specificity for PD173074 in vivo is unclear; thus, it likely has nonspecific antagonism of other FGFRs. Future studies should investigate the specific roles of FGFRs, their isoforms, and their neuronal effectors in central regulation of metabolism by performing selective deletion of FGFRs in specific neurons of mature mice using the inducible Cre-LoxP system.

In addition to FGFR-PI3K signaling, there are likely unknown concurrent mechanisms underlying central α-klotho–mediated metabolic regulation. Other neuron populations, such as proopiomelanocortin (POMC) neurons, which are closely associated with NPY/AgRP neurons, may be involved. Our cell culture and immunohistochemistry data also may suggest ERK as an additional cell signaling mechanism of hypothalamic α-klotho action. ERK signaling is downstream of α-klotho, negatively regulates NPY/AgRP neurons, possibly via Kruppel-like factor 4, and is involved in hypothalamic FGF1- and FGF19-mediated glucose lowering (21,43,48).

To summarize, this study identifies α-klotho as a novel antagonist of NPY/AgRP neurons and demonstrates α-klotho's importance to central regulation of metabolism via an α-klotho–FGFR1–PI3K signaling axis. Our data revealed central administration of α-klotho to yield various therapeutic effects in models of type 1 and 2 diabetes, including improved glucose regulation, suppressed food intake, and reduced body weight. To our knowledge, this study provides the first evidence of α-klotho as a novel hypothalamic regulator of energy balance and glucose metabolism, thus providing new insight into the pathophysiology of metabolic disease.

Duality of Interest. No potential conflicts of interest relevant to this article were reported.

References

1. Kurosu H, Yamamoto M, Clark JD, et al. Suppression of aging in mice by the hormone klotho. Science 2005;309:1829–1833

2. Olauson H, Mencke R, Hillebrands J-L, Larsson TE. Tissue expression and source of circulating αKlotho. Bone 2017;100:19–35

3. Lin Y, Sun Z. Antiaging gene klotho attenuates pancreatic β-cell apoptosis in type 1 diabetes. Diabetes 2015;64:4298–4311

4. Lin Y, Sun Z. Antiaging gene Klotho enhances glucose-induced insulin secretion by up-regulating plasma membrane levels of TRPV2 in MIN6 β-cells. Endocrinology 2012;153:3029–3039

5. Lin Y, Sun Z. In vivo pancreatic β-cell-specific expression of antiaging gene Klotho: a novel approach for preserving β-cells in type 2 diabetes. Diabetes 2015; 64:1444–1458

6. Rao Z, Landry T, Li P, et al. Administration of alpha klotho reduces liver and adipose lipid accumulation in obese mice. Heliyon 2019;5:e01494

7. Mori K, Yahata K, Mukoyama M, et al. Disruption of klotho gene causes an abnormal energy homeostasis in mice. Biochem Biophys Res Commun 2000;278: 665–670

8. Nie F, Wu D, Du H, et al. Serum klotho protein levels and their correlations with the progression of type 2 diabetes mellitus. J Diabetes Complications 2017; 31:594–598

9. Leon J, Moreno AJ, Garay BI, et al. Peripheral elevation of a klotho fragment enhances brain function and resilience in young, aging, and α-synuclein transgenic mice. Cell Rep 2017;20:1360–1371

10. Zeldich E, Chen C-D, Colvin TA, et al. The neuroprotective effect of Klotho is mediated via regulation of members of the redox system. J Biol Chem 2014;289: 24700–24715

11. Chen C-D, Sloane JA, Li H, et al. The antiaging protein Klotho enhances oligodendrocyte maturation and myelination of the CNS. J Neurosci 2013;33: 1927–1939

12. Chen L-J, Cheng M-F, Ku P-M, Cheng J-T. Cerebral klotho protein as a humoral factor for maintenance of baroreflex. Horm Metab Res 2015;47:125–132

13. Nakajima K, Cui Z, Li C, et al. Gs-coupled GPCR signalling in AgRP neurons triggers sustained increase in food intake. Nat Commun 2016;7:10268

14. Könner AC, Janoschek R, Plum L, et al. Insulin action in AgRP-expressing neurons is required for suppression of hepatic glucose production. Cell Metab 2007;5:438–449

15. Krashes MJ, Shah BP, Madara JC, et al. An excitatory paraventricular nucleus to AgRP neuron circuit that drives hunger. Nature 2014;507:238–242

16. Tong Q, Ye C-P, Jones JE, Elmquist JK, Lowell BB. Synaptic release of GABA by AgRP neurons is required for normal regulation of energy balance. Nat Neurosci 2008;11:998–1000

17. Wang Q, Liu C, Uchida A, et al. Arcuate AgRP neurons mediate orexigenic and glucoregulatory actions of ghrelin. Mol Metab 2013;3:64–72

18. Korner J, Savontaus E, Chua SC Jr., Leibel RL, Wardlaw SL. Leptin regulation of Agrp and Npy mRNA in the rat hypothalamus. J Neuroendocrinol 2001;13:959–966

19. Qu SY, Yang YK, Li JY, Zeng Q, Gantz I. Agouti-related protein is a mediator of diabetic hyperphagia. Regul Pept 2001;98:69–75

20. Morton GJ, Matsen ME, Bracy DP, et al. FGF19 action in the brain induces insulin-independent glucose lowering. J Clin Invest 2013;123:4799–4808

21. Marcelin G, Jo Y-H, Li X, et al. Central action of FGF19 reduces hypothalamic AGRP/NPY neuron activity and improves glucose metabolism. Mol Metab 2013;3: 19–28

22. Sarruf DA, Thaler JP, Morton GJ, et al. Fibroblast growth factor 21 action in the brain increases energy expenditure and insulin sensitivity in obese rats. Diabetes 2010;59:1817–1824

23. Rojas JM, Matsen ME, Mundinger TO, et al. Glucose intolerance induced by blockade of central FGF receptors is linked to an acute stress response. Mol Metab 2015;4:561–568

24. Owen BM, Ding X, Morgan DA, et al. FGF21 acts centrally to induce sympathetic nerve activity, energy expenditure, and weight loss. Cell Metab 2014; 20:670–677

25. Al-Qassab H, Smith MA, Irvine EE, et al. Dominant role of the p110β isoform of PI3K over p110α in energy homeostasis regulation by POMC and AgRP neurons. Cell Metab 2009;10:343–354

26. Kurosu H, Ogawa Y, Miyoshi M, et al. Regulation of fibroblast growth factor-23 signaling by klotho. J Biol Chem 2006;281:6120–6123

27. Chen G, Liu Y, Goetz R, et al. α-Klotho is a non-enzymatic molecular scaffold for FGF23 hormone signalling. Nature 2018;553:461–466

28. Hensel N, Schön A, Konen T, et al. Fibroblast growth factor 23 signaling in hippocampal cells: impact on neuronal morphology and synaptic density. J Neurochem 2016;137:756–769

29. Pardo OE, Latigo J, Jeffery RE, et al. The fibroblast growth factor receptor inhibitor PD173074 blocks small cell lung cancer growth in vitro and in vivo. Cancer Res 2009;69:8645–8651

30. Rahmouni K, Haynes WG, Morgan DA, Mark AL. Intracellular mechanisms involved in leptin regulation of sympathetic outflow. Hypertension 2003;41:763–767

31. Laing BT, Do K, Matsubara T, et al. Voluntary exercise improves hypothalamic and metabolic function in obese mice. J Endocrinol 2016;229:109–122

32. Laing BT, Li P, Schmidt CA, et al. AgRP/NPY neuron excitability is modulated by metabotropic glutamate receptor 1 during fasting. Front Cell Neurosci 2018;12: 276

33. Ting JT, Daigle TL, Chen Q, Feng G. Acute brain slice methods for adult and aging animals: application of targeted patch clamp analysis and optogenetics. Methods Mol Biol 2014;1183:221–242

34. Qiu J, Rivera HM, Bosch MA, et al. Estrogenic-dependent glutamatergic neurotransmission from kisspeptin neurons governs feeding circuits in females. Elife 2018;7:e35656

35. Katayama J, Akaike N, Nabekura J. Characterization of pre- and post-synaptic metabotropic glutamate receptor-mediated inhibitory responses in substantia nigra dopamine neurons. Neurosci Res 2003;45:101–115

36. Mellon PL, Windle JJ, Goldsmith PC, Padula CA, Roberts JL, Weiner RI. Immortalization of hypothalamic GnRH neurons by genetically targeted tumorigenesis. Neuron 1990;5:1–10

37. Chen GJ, Weylie B, Hu C, Zhu J, Forough R. FGFR1/PI3K/AKT signaling pathway is a novel target for antiangiogenic effects of the cancer drug fumagillin (TNP-470). J Cell Biochem 2007;101:1492–1504

38. Li X, Li Z, Li B, Zhu X, Lai X. Klotho improves diabetic cardiomyopathy by suppressing the NLRP3 inflammasome pathway. Life Sci 2019;234:116773

39. Wan Q, He Y, Yuan M. Klotho in diabetes and diabetic nephropathy: a brief update review. Int J Clin Exp Med 2017;10:4342–4349

40. Krashes MJ, Koda S, Ye C, et al. Rapid, reversible activation of AgRP neurons drives feeding behavior in mice. J Clin Invest 2011;121:1424–1428

41. Ahren B, Wierup N, Sundler F. Neuropeptides and the regulation of islet function. Diabetes 2006;55:S98–S107

42. Gil SY, Youn B-S, Byun K, et al. Clusterin and LRP2 are critical components of the hypothalamic feeding regulatory pathway. Nat Commun 2013;4:1862

43. Park M, Oh H, York DA. Enterostatin affects cyclic AMP and ERK signaling pathways to regulate Agouti-related protein (AgRP) expression. Peptides 2009;30: 181–190

44. Ryan KK, Kohli R, Gutierrez-Aguilar R, Gaitonde SG, Woods SC, Seeley RJ. Fibroblast growth factor-19 action in the brain reduces food intake and body weight and improves glucose tolerance in male rats. Endocrinology 2013;154:9–15

45. Samms RJ, Lewis JE, Lory A, et al. Antibody-mediated inhibition of the FGFR1c isoform induces a catabolic lean state in Siberian hamsters. Curr Biol 2015;25:2997–3003

46. Sun HD, Malabunga M, Tonra JR, et al. Monoclonal antibody antagonists of hypothalamic FGFR1 cause potent but reversible hypophagia and weight loss in rodents and monkeys. Am J Physiol Endocrinol Metab 2007;292:E964–E976

47. Liu S, Marcelin G, Blouet C, et al. A gut-brain axis regulating glucose metabolism mediated by bile acids and competitive fibroblast growth factor actions at the hypothalamus. Mol Metab 2018;8:37–50

48. Brown JM, Scarlett JM, Matsen ME, et al. The hypothalamic arcuate nucleus-median eminence is a target for sustained diabetes remission induced by fibroblast growth factor 1. Diabetes 2019;68:1054–1061